



# A boundary element method for dynamic plate bending problems

P.H. Wen<sup>a</sup>, M.H. Aliabadi<sup>a,\*</sup>, A. Young<sup>b</sup>

<sup>a</sup>*Department of Engineering, Queen Mary and Westfield College, London University, E1 4NS, London, UK*

<sup>b</sup>*Structural Materials Centre, DERA, Farnborough, Hants GU14 6TD, UK*

Received 19 February 1999; in revised form 15 June 1999

---

## Abstract

In this paper the fundamental solution for Kirchhoff plate in the Laplace transform domain is deduced and the boundary element formulation is established to study plate bending problem. By use of the moment integral equation, the dual boundary element equation is developed to solve the cracked plate problem subjected to dynamic loads. Durbin's Laplace transform inversion method is used and the dynamic stress intensity factors are determined by equivalent stress technique. An infinite plate containing an isolated crack or two cracks, or one set of parallel cracks under Heaviside load on the crack surfaces is studied. The numerical results obtained demonstrate the efficiency and accuracy of the proposed formulation. © 2000 Elsevier Science Ltd. All rights reserved.

*Keywords:* Boundary element method; Plate bending; Dynamic stress intensity factors

---

## 1. Introduction

Thin plate structures are widely used in analysing engineering structures. Numerical methods such as the finite element method and finite difference method are well established in plate bending problems. An early application of the boundary integral equation to the plate bending problem is due to Jaswon and Maiti (1968). Later indirect boundary integral equation solutions of Kirchhoff plate bending problems were presented by Altirero and Sikarskie (1978) and Tottenham (1979). Direct boundary integral formulations can be found in papers by several authors (see Maiti and Chakrabarty, 1974; Stern, 1981; Du and Lu, 1986). For Reissner plate model, the boundary integral equation was reported by Vander Weeën (1982), who used the Hormander method to deduce the fundamental solution.

---

\* Corresponding author. Tel.: +44-171-975-5190; fax: +44-181-983-3052.

E-mail address: M.H.Aliabadi@qmw.ac.uk (M.H. Aliabadi).

The applications of boundary element method to the dynamic analysis for plate bending problem were presented by Bezin (1991). The mass matrix technique widely used by finite element method was employed to deal with the dynamic response problems. Readers should consult Beskos (1991) for recent developments in dynamics. A comprehensive description of recent advances in BEM in plate bending can be found in Ref. (Aliabadi, 1998).

In this paper the fundamental solution for Kirchhoff plate in the Laplace transform domain is derived and the dual boundary integral equation is presented for the first time. By the use of moment integral equation on the crack surface, the discontinuity displacement (slop) can be determined which can be used to evaluate the stress intensity factors at the crack tip. The choice of a special set of Laplace transform parameters in the transform domain allows the displacements in the time domain to be obtained by Durbin's inversion method (Durbin, 1974). Some numerical examples are presented to demonstrate the application of the proposed method.

## 2. Fundamental solution

Consider an infinite Kirchhoff plate subjected to a concentrated force  $\delta(t)$  at the origin, the governing equation in polar coordinate system  $(r, \theta)$  can be written as

$$\nabla^2 \nabla^2 w^* + \frac{\rho h}{D} \frac{\partial^2 w^*}{\partial t^2} = \delta(t) \delta(r) \quad (1)$$

where  $D = Eh^3/12(1 - \nu^2)$ ,  $E$  and  $\nu$  are the elastic constants,  $t$  is the time and  $\nabla^2$  is harmonic operator defined by

$$\nabla^2 = \frac{\partial^2}{\partial r^2} + \frac{1}{r} \frac{\partial}{\partial r}.$$

Taking Laplace transforms, Eq. (1) becomes

$$\nabla^2 \nabla^2 \tilde{w}^* + \frac{\rho h s^2}{D} \tilde{w}^* = \delta(r) \quad (2)$$

where  $s$  is the Laplace transform parameter. This governing equation is the same as that for plate resting on the Winkler model foundation. The fundamental solution for Eq. (2) can be obtained as

$$\tilde{w}^*(s, r) = \frac{l^2}{4D} f_0(\xi) \quad (3)$$

where

$$f_0(\xi) = -\frac{1}{\pi} [K_0(\xi\sqrt{i}) - K_0(\xi\sqrt{-i})]$$

and its series expansion is listed in Appendix A, where  $i = \sqrt{-1}$ ,  $\xi = r/l$  and  $l = (D/\rho h s^2)^{1/4}$ . Thus the fundamental solution can be rearranged as

$$\tilde{w}^*(s, r) = -\frac{1}{4\pi i} \sqrt{\frac{D}{\rho h s}} [K_0(\xi\sqrt{i}) - K_0(\xi\sqrt{-i})] \quad (4)$$

By Laplace transform inversion formula, the fundamental solution in time domain can be obtained as

$$w^*(t, r) = \frac{1}{8\pi} \sqrt{\frac{D}{\rho h}} \operatorname{si} \left( \sqrt{\frac{\rho h r^2}{D 4t}} \right) \tag{5}$$

where  $\operatorname{si}(u)$  is sine integral and defined as

$$\operatorname{si}(u) = \int_u^\infty \frac{\sin u}{u} \, du.$$

### 3. Boundary element method in Laplace transform domain

Consider an isotropic elastic plate  $\Omega$  enclosed by boundary  $\Gamma$ . The out-of-plane transformed boundary conditions are given as:

$$w(s) = \bar{w}(s) \quad \text{or} \quad V_n(s) = \bar{V}_n(s) \tag{6}$$

$$\theta(s) = \frac{\partial w}{\partial n} = \frac{\partial \bar{w}}{\partial n} \quad \text{or} \quad M_n(s) = \bar{M}_n(s) \tag{7}$$

where

$$V_n(s) = -D \frac{\partial}{\partial n} (\nabla^2 w) + \frac{\partial M_\tau}{\partial \tau}$$

$$M_n(s) = -D \left[ (n_1^2 + \nu n_2^2) \frac{\partial^2 w}{\partial x^2} + 2(1 - \nu) n_1 n_2 \frac{\partial^2 w}{\partial x \partial y} + (n_2^2 + \nu n_1^2) \frac{\partial^2 w}{\partial y^2} \right]$$

$$M_\tau(s) = -D(1 - \nu) \left[ (n_1^2 - n_2^2) \frac{\partial^2 w}{\partial x \partial y} + n_1 n_2 \left( \frac{\partial^2 w}{\partial x^2} - \frac{\partial^2 w}{\partial y^2} \right) \right]$$

and  $n$  and  $\tau$  are directions normal and tangential, respectively. The deflection at a domain point  $\mathbf{X}'$  in  $\Omega$  can be determined from the boundary values of moment and deflection through Betti's reciprocity principle as

$$Dw(\mathbf{X}') = \int_\Gamma \tilde{w}^*(\mathbf{X}', \mathbf{x}') V_n(\mathbf{x}') \, d\Gamma + \int_\Gamma \tilde{M}_n^*(\mathbf{X}', \mathbf{x}') \theta(\mathbf{x}') \, d\Gamma - \int_\Gamma \tilde{V}_n^*(\mathbf{X}', \mathbf{x}') w(\mathbf{x}') \, d\Gamma - \int_\Gamma \tilde{\theta}^*(\mathbf{X}', \mathbf{x}') M_n(\mathbf{x}') \, d\Gamma + \int_\Omega \tilde{w}^*(\mathbf{X}', \mathbf{X}) q(\mathbf{X}) \, d\Omega \tag{8}$$

where  $q(\mathbf{X})$  is the distributed normal load intensity in domain. The moments in the domain, for instance moment  $M_y$ , can be determined by following equation

$$M_y = -D \left( \frac{\partial^2 w}{\partial y^2} + \nu \frac{\partial^2 w}{\partial x^2} \right) = -D \nabla_y^2 w(\mathbf{X}') \tag{9}$$

where

$$\nabla_y^2 = \frac{\partial^2}{\partial y^2} + \nu \frac{\partial^2}{\partial x^2}$$

From the boundary integral equation (8), the moment equation becomes

$$\begin{aligned} M_y(\mathbf{X}') = & - \int_{\Gamma} \nabla_y^2 \tilde{w}^*(\mathbf{X}', \mathbf{x}') V_n(\mathbf{x}') d\Gamma - \int_{\Gamma} \nabla_y^2 \tilde{M}_n^*(\mathbf{X}', \mathbf{x}') \theta(\mathbf{x}') d\Gamma + \int_{\Gamma} \nabla_y^2 \tilde{V}_n^*(\mathbf{X}', \mathbf{x}') w(\mathbf{x}') d\Gamma \\ & + \int_{\Gamma} \nabla_y^2 \tilde{\theta}^*(\mathbf{X}', \mathbf{x}') M_n(\mathbf{x}') d\Gamma - \int_{\Omega} \nabla_y^2 \tilde{w}^*(\mathbf{X}', \mathbf{X}) q(\mathbf{X}) d\Omega \end{aligned} \quad (10)$$

The deflection and moment boundary integral equations for the point on the external boundary  $\Gamma$  can be obtained from Eq. (8) by considering the limit as the domain point  $\mathbf{X}' \rightarrow \mathbf{x}'$  on the boundary. The same procedure as illustrated by Aliabadi and Rooke (1991) can be used to obtain the boundary integrals in the Laplace domain, for a smooth boundary, it can be written as

$$\begin{aligned} \frac{1}{2} Dw(\mathbf{x}') = & \int_{\Gamma} \tilde{w}^*(\mathbf{x}', \mathbf{x}') V_n(\mathbf{x}') d\Gamma + \int_{\Gamma} \tilde{M}_n^*(\mathbf{x}', \mathbf{x}') \theta(\mathbf{x}') d\Gamma - \int_{\Gamma} \tilde{V}_n^*(\mathbf{x}', \mathbf{x}') w(\mathbf{x}') d\Gamma \\ & - \int_{\Gamma} \tilde{\theta}^*(\mathbf{x}', \mathbf{x}') M_n(\mathbf{x}') d\Gamma + \int_{\Omega} \tilde{w}^*(\mathbf{x}', \mathbf{X}) q(\mathbf{X}) d\Omega \end{aligned} \quad (11)$$

for deflection, where  $\int$  denotes a Cauchy principal-value integral and

$$\begin{aligned} M_n(\mathbf{x}') = & - \int_{\Gamma} \nabla_n^2 \tilde{w}^*(\mathbf{x}', \mathbf{x}') V_n(\mathbf{x}') d\Gamma - \int_{\Gamma} \nabla_n^2 \tilde{M}_n^*(\mathbf{x}', \mathbf{x}') \theta(\mathbf{x}') d\Gamma + \int_{\Gamma} \nabla_n^2 \tilde{V}_n^*(\mathbf{x}', \mathbf{x}') w(\mathbf{x}') d\Gamma \\ & + \int_{\Gamma} \nabla_n^2 \tilde{\theta}^*(\mathbf{x}', \mathbf{x}') M_n(\mathbf{x}') d\Gamma - \int_{\Omega} \nabla_n^2 \tilde{w}^*(\mathbf{x}', \mathbf{X}) q(\mathbf{X}) d\Omega \end{aligned} \quad (12)$$

where  $\int$  denotes a Hadamard principal-value integral (see Hadamard, 1923) and the operator  $\nabla_n^2$  is defined by

$$\nabla_n^2 = (n_1^2 + \nu n_2^2) \frac{\partial^2}{\partial x^2} + 2(1 - \nu) n_1 n_2 \frac{\partial^2}{\partial x \partial y} + (n_2^2 + \nu n_1^2) \frac{\partial^2}{\partial y^2}$$

For the pure model I crack bending problem, Eqs. (10) and (11) are sufficient. By applying the deflection integral equation on one of the crack surfaces and the moment boundary integral equation on the other, a pure model I crack problem can be solved in a single region as illustrated by Fedelinski et al. (1995). For the mixed mode problems, the reduced Kirchhoff force boundary integral equation should be considered.

#### 4. Discontinuity slop equation and stress intensity factor evaluation

Consider an infinite plate containing a crack with the length  $2a$  subjected to the bending moment  $M_0(x')f(t)$  on crack surfaces as shown in Fig. 1. Considering the relationship:

$$\tilde{M}_n^* = \tilde{M}_y^* = -D \nabla_y^2 \tilde{w}^*, \quad \nabla_n^2 = \nabla_y^2$$

the moment Eq. (12) becomes:

$$M_n(x') = \int_{\Gamma} D \nabla_y^2 \nabla_y^2 \tilde{w}^*(x' - x) [\theta(x^+) - \theta(x^-)] dx \tag{13}$$

where  $\theta(x^+)$  and  $\theta(x^-)$  are slopes on the crack surface. Let  $\Delta\theta(x) = \theta(x^+) - \theta(x^-)$  be the discontinuity of slope and consider the moment condition on crack surface, Eq. (13) gives

$$\int_{\Gamma} D \nabla_y^2 \nabla_y^2 \tilde{w}^*(x' - x) \Delta\theta(x) dx = M_0(x') f(s) \tag{14}$$

where

$$f(s) = \int_0^{\infty} f(t) e^{-st} dt.$$

To solve the above integral equation, constant elements are used in the numerical calculation as shown by Wen et al. (1996a, 1996b) for two-dimensional and three-dimensional problems respectively. First, the crack is divided into  $N$  straight segments and the mid-point of each segment is defined by coordinate  $(x')$ . Using this discretization for the moment Eq. (14), the integral equation for each element  $m$  becomes:

$$\sum_{n=1}^N A_{mn} \Delta\theta^n = M_0(x'_m) f(s) \tag{15}$$

where

$$A_{mn} = \int_{\Delta\Gamma_n} D \nabla_y^2 \nabla_y^2 \tilde{w}^*(x'_m - x) dx$$

and can be determined numerically by an infinite integral as shown in Appendix B. By solving the above equations, the discontinuities of slope for each element can be evaluated numerically.

For constant elements, the equivalent stress technique can be used to obtain accurate stress intensity factors, see Wen et al. (1996a, 1996b). For static Kirchhoff bending problem, the fundamental solution is

$$w^*(r) = r^2 \ln r \tag{16}$$

$$A_{mn}^{st} = \frac{(3 + \nu)(1 - \nu)D}{\pi} \frac{\lambda}{(x'_m - x'_n)^2 - \lambda^2} \tag{17}$$

where  $\lambda$  is the half-length of element ( $\lambda = a/N$ ). Because the singularity fields for stresses in the Laplace

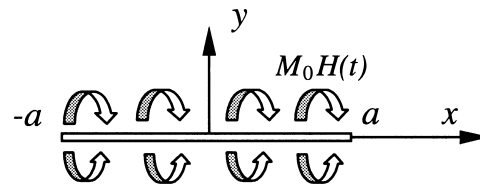


Fig. 1. An isolated crack subjected to impact load.

transform domain at a crack tip are the same as in elastostatic problems, the equivalent stress can be written as

$$M_m^0(s) = \sum_{n=1}^N A_{mn}^{st} \Delta\theta^n(s) \quad (18)$$

From the Green's function formula for stress intensity factor (see Wen, 1996), it follows that

$$K_I(s)(\pm a) = \frac{1}{\sqrt{\pi a}} \int_{-a}^a M^0(x) \sqrt{\frac{a \pm x}{a \mp x}} dx = \sum_{n=1}^N \sum_{m=1}^N A_{mn}^{st} F_n(\pm a) \Delta\theta^m \sqrt{\pi a} \quad (19)$$

where

$$F_n(\pm a) = \frac{1}{\pi} \left[ \arcsin\left(\frac{x}{a}\right) \mp \sqrt{1 - \frac{x}{a}} \right]_{x_n - \lambda}^{x_n + \lambda}$$

From above equation, it can be seen that the stress intensity factor depends on the discontinuity slopes of all crack elements and not just the elements close to the crack tip. However, the closer to the crack tip an element is, the greater is its influence. The time-dependent stress intensity factor can be obtained by an inverse transform, see Durbin (1974). The formula used is as follows

$$K_I(t) = 2 \frac{e^{ct}}{T} \left( -\frac{1}{2} \operatorname{Re}[\tilde{K}_I(c)] + \sum_{k=0}^L \operatorname{Re}[\tilde{K}_I(s_k)] \cos \frac{2k\pi t}{T} - \sum_{k=0}^L \operatorname{Im}[\tilde{K}_I(s_k)] \sin \frac{2k\pi t}{T} \right) \quad (20)$$

where  $\tilde{K}_I(s)$  stands for the value in Laplace space at the sample point  $s_k = c + 2k\pi i/T$ . The sample points are chosen for  $k = 0, 1, \dots, L$ . Accurate results have been obtained for  $cT = 5$  and  $T/t_0 = 20$ , where  $t_0 = a/c_2$  is unit time.

## 5. Numerical example

To demonstrate the accuracy of the above method, several numerical examples under dynamic load are studied in this section. The first example shows the application to an isolated crack in an infinite domain subjected to uniform impact load  $M_0 H(t)$ . The second and the third examples demonstrate the application to two collinear cracks and a periodic parallel cracks under the impact load. The normalized dynamic stress intensity factors  $K_I(t)/M_0\sqrt{\pi a}$  versus the normalized time  $c_2 t/a$  for Poisson's ratio  $\nu = 0.25$  are presented, where  $c_2 = \sqrt{G/\rho}$  is the velocity of elastic shear wave and  $G$  is elasticity constant.

### 5.1. Example 1: isolated crack under impact load

An isolated crack of length  $2a$  in an infinite sheet subjected to a uniform impact load  $M_0 H(t)$  is shown in Fig. 1, where  $H(t)$  is the Heaviside function. The number of elements  $N = 10$  and the number of sample points in Laplace transform domain  $L = 200$ . The normalized dynamic moment intensity factor  $F(t)$  to static value  $M_0\sqrt{\pi a}$  for the different ratios  $a/h$  are shown in Fig. 2. Unlike the two-dimensional and three-dimensional elastodynamic cracked bodies (see Wen et al., 1996a, 1996b), the dynamic moment intensity factor increases with time and approach the static value (1.0) smoothly. Decreasing plate thickness tends to lower the  $K_I(t)$  value. The relative error between the solutions for

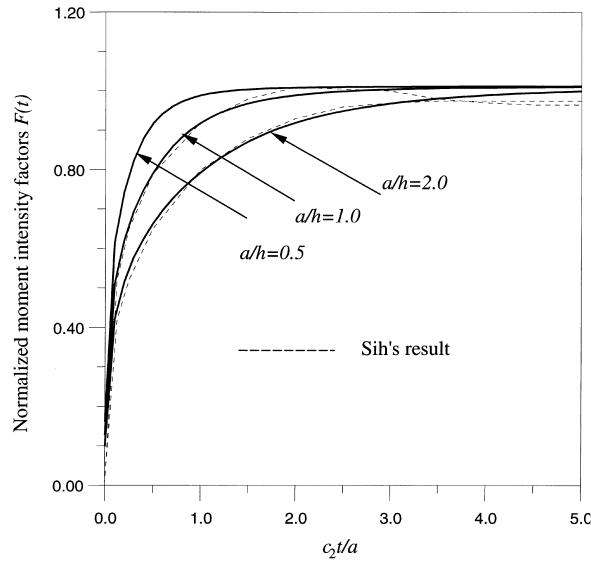


Fig. 2. Dynamic moment intensity factors for different ratios  $a/h$ .

different element number  $N > 10$  are very small. Sih and Chen (1977) results of time dependent moment intensity factor are plotted in the figure for comparison.

5.2. Example 2: two collinear cracks under impact load

Two collinear cracks AB and CD are shown in Fig. 3 with a uniform impact moment  $M_0H(t)$  acting on one of the crack surfaces (left). The length of each crack is  $2a$  and the distance between two crack centres is  $d$ . The number of elements  $N = 10$  and the number of sample point in Laplace transform domain  $L = 200$ . The normalized moment intensity factors  $F_A, F_B$  are almost the same as that in Example 1. For the free crack CD, the normalized factors  $F_C$  and  $F_D$  to  $K^0 = M_0\sqrt{\pi a}$  at points C and D are shown in Fig. 4 for different ratios  $a/h$  against the normalized time  $c_2t/a$ . Because the moment intensity factors  $F_A$  and  $F_B$  are the same for small time  $t$ , it means that the interaction between two cracks is very small. The dynamic moment intensity factors are very smooth and approach the static values. When the dynamic load are applied on the both crack surfaces, the moment intensity factors at point A and B are shown in Fig. 5. In this case the static values can be written as (see Isida, 1977)

$$F_B^{st} = \frac{1}{2\lambda}(1 - \lambda)^{1/2} \left[ (1 + \lambda)^2 \frac{E(m)}{K(m)} - (1 - \lambda)^2 \right]$$

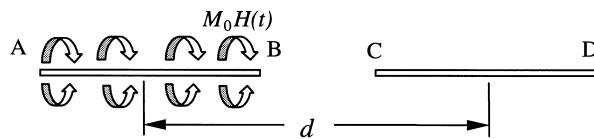


Fig. 3. Collinear cracks subjected to impact load.

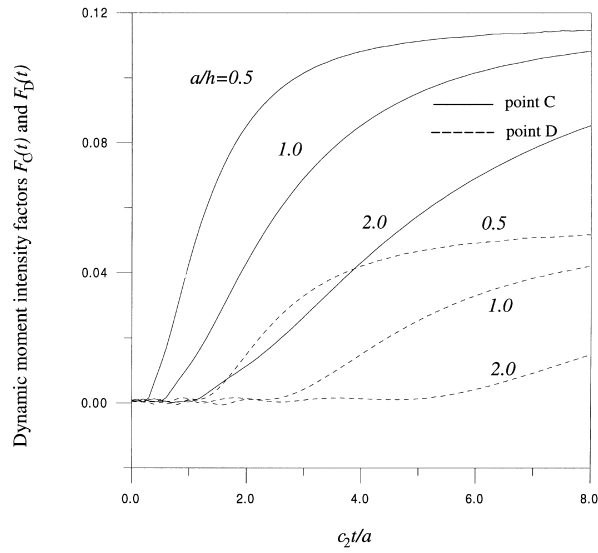


Fig. 4. Moment intensity factors at points C and D for collinear cracks.

$$F_A^{st} = \frac{(1 + \lambda)^{3/2}}{2\lambda} \left[ 1 - \frac{E(m)}{K(m)} \right]$$

where  $m = 2\sqrt{\lambda}/(1 + \lambda)$ ,  $\lambda = 2a/d$  and  $E(m)$ ,  $K(m)$  are complete elliptic integrals of the first and second kinds respectively. If  $d = 3a$ ,  $\lambda = 2/3$ ,  $m = 0.9798$ , the static moment intensity factors are  $F_A^{st} = 1.0524$  and  $F_B^{st} = 1.1111$ .

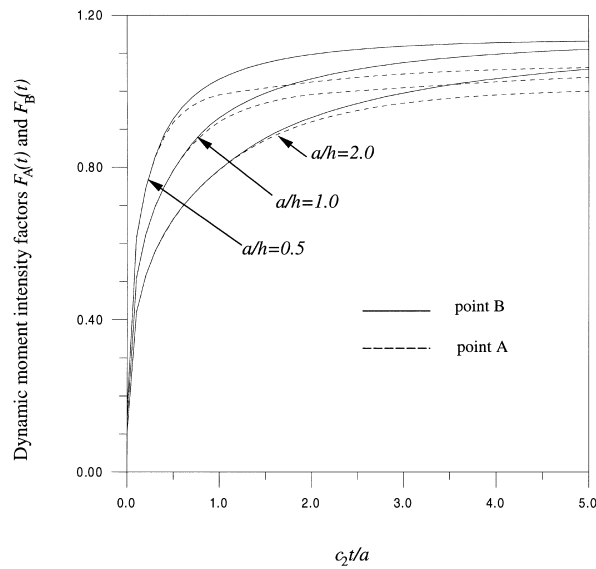


Fig. 5. Results for collinear cracks at points A and B for impact load on two cracks.



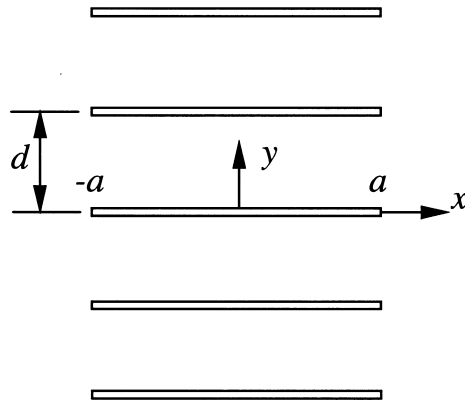


Fig. 6. Periodic parallel cracks.

5.3. Example 3: periodic parallel cracks under impact load

Periodic parallel cracks of length  $2a$  in an infinite sheet subjected to a uniform impact load  $M_0H(t)$  is shown in Fig. 6, the distance between cracks is  $d$ . The number of elements and the number of sample point in Laplace transform domain are the same as in above examples. The normalized dynamic moment intensity factors for the  $\lambda = 2a/d = 0.5, 0.9$  and  $2$  with ratio  $a/h = 1$  are shown in Fig. 7. In this case, the interaction between cracks is very large and the dynamic moment intensity factors oscillate about the static values.

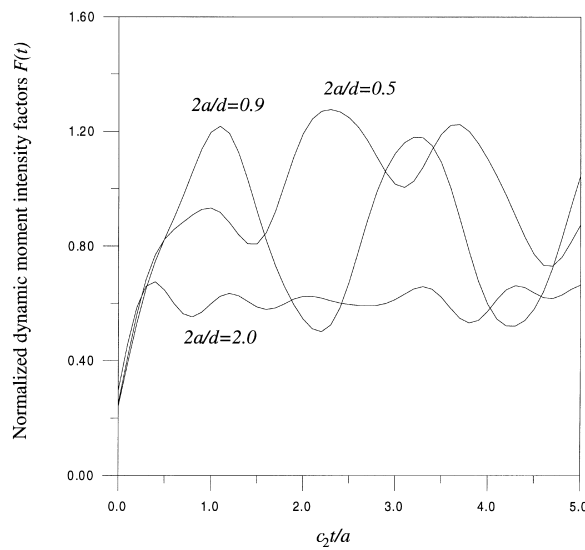


Fig. 7. Results for Periodic parallel cracks under impact load.

## 6. Conclusion

The problem of cracks in plate bending subjected to dynamic loading was studied by boundary element method in the Laplace transform domain. Dual boundary integral equations for crack bending problems were established by Betti's reciprocity principle. For an infinite plate problem with straight cracks, the integral equations contain only unknown of discontinuity slope. By use of constant element and equivalent stress technique, the moment intensity factors can be determined with high accuracy.

## Acknowledgements

This work has been carried out with the support of the Ministry of Defence, Defence Evaluation and Research Agency, FARNBOROUGH, Hants, U.K.

## Appendix A. Functions of fundamental solution

Because the Bessel function  $K_0(z)$  can be written as

$$K_0(z) = \sum_{k=0}^{\infty} \frac{z^{2k}}{2^{2k}(k!)^2} \sum_{m=1}^k \frac{1}{m} - \left( \ln \frac{z}{2} + \gamma \right) I_0(z) \quad (\text{A.1})$$

where

$$I_0(z) = \sum_{k=0}^{\infty} \frac{z^{2k+1}}{2^{2k+1} k!(k+1)!}$$

and  $\gamma = 0.577215664$  is Euler's constant. Thus

$$f_0(\xi) = -\frac{1}{\pi i} [K_0(\sqrt{i\xi}) - K_0(\sqrt{-i\xi})] = \frac{1}{2} Z_1(u) - \frac{2}{\pi} \left[ R(u) + \left( \frac{1}{2} \ln u + \gamma \right) Z_2(u) \right] \quad (\text{A.2})$$

where

$$Z_1 = 1 - \frac{u^2}{(2!)^2} + \frac{u^4}{(4!)^2} - \frac{u^6}{(6!)^2} + \dots$$

$$R(u) = u - \frac{1}{(3!)^2} \left( 1 + \frac{1}{2} + \frac{1}{3} \right) u^3 + \frac{1}{(5!)^2} \left( 1 + \frac{1}{2} + \frac{1}{3} + \frac{1}{5} \right) u^5 - \dots$$

$$Z_2(u) = -u + \frac{u^3}{(3!)^2} - \frac{u^5}{(5!)^2} + \dots$$

$$u = \frac{r^2}{4l^2}$$

The fundamental solution in Eq. (13) can be written as

$$\begin{aligned} \nabla_y^2 \nabla_y^2 \tilde{w}^* &= \frac{l^2}{4} \left( \frac{\partial^4 f_0}{\partial y^4} + 2\nu \frac{\partial^4 f_0}{\partial y^2 \partial x^2} + \nu^2 \frac{\partial^4 f_0}{\partial x^4} \right) \\ &= \frac{1}{64l^2} \left[ 4(3 + 2\nu + 3\nu^2) f^{(2)} + \frac{4[3y^2 + \nu(y^2 + x^2) + \nu^2 x^2]}{l^2} f^{(3)} + \frac{(y^2 + \nu x^2)^2}{l^4} f^{(4)} \right] \end{aligned} \quad (A.3)$$

where

$$f^{(n)} = \frac{\partial^n f(u)}{\partial u^n}, \quad \frac{\partial u}{\partial x} = \frac{x}{2l}, \quad \frac{\partial u}{\partial y} = \frac{y}{2l}$$

### Appendix B. Matrix coefficients

From Eq. (15), the Bessel's function  $K_0(z)$  should be used to determine the coefficient  $A_{nm}$ . Consider the following integral relation

$$K_0(\beta r) = \int_0^\infty \frac{\cos \omega x}{\sqrt{\omega^2 + \beta^2}} e^{-\sqrt{\omega^2 + \beta^2} y} d\omega \quad (B.1)$$

Thus for constant elements

$$\begin{aligned} A_{nm} &= A_{nm}(x_m - x_n, y) = \int_{x_n - \lambda}^{x_n + \lambda} D \nabla_y^2 \nabla_y^2 \tilde{w}^*(x_m - x, y) dx = \frac{D}{\beta^2} \\ &\int_0^\infty \left\{ \sqrt{\omega^2 + \beta^2} [(1 - \nu)\omega^2 + \beta^2] e^{-\sqrt{\omega^2 + \beta^2} y} - \sqrt{\omega^2 - \beta^2} [(1 - \nu)\omega^2 \right. \\ &\quad \left. - \beta^2] e^{-\sqrt{\omega^2 - \beta^2} y} \right\} \frac{\sin \lambda \omega}{\omega} \cos(x_m - x_n) \omega d\omega + \frac{\nu D}{\beta^2} \\ &\int_0^\infty \left\{ \frac{(1 - \nu)\omega^2 + \beta^2}{\sqrt{\omega^2 + \beta^2}} e^{-\sqrt{\omega^2 + \beta^2} y} - \frac{(1 - \nu)\omega^2 - \beta^2}{\sqrt{\omega^2 - \beta^2}} e^{-\sqrt{\omega^2 - \beta^2} y} \right\} \omega \sin \lambda \omega \cos(x_m - x_n) \omega d\omega \end{aligned} \quad (B.2)$$

where  $\beta^2 = is\sqrt{\rho h/D}$ . It is simple to obtain the numerical values of  $A_{nm}$  for given Laplace transform parameter  $s_k$ . For periodic parallel cracks as shown in Example 3, the coefficient  $A_{nm}$  should be considered as the contribution by all elements on each crack and can be written as

$$A_{nm} = A_{nm}(x_m - x_n, 0) + 2 \sum_{k=1}^\infty A_{nm}(x_m - x_n, kd)$$

where  $d$  is the distance between two crack centers.

### References

Aliabadi, M.H., 1998. Plate Bending Analysis with Boundary Elements. Computational Mechanics Publications, Southampton UK, Boston USA.

- Aliabadi, M.H., Rooke, D.P., 1991. *Numerical Fracture Mechanics*. Computational Mechanics Publications/Kluwer Academic Publishers, Southampton UK, Boston, USA/Dordrecht.
- Altirero, N.J., Sikarskie, D.L., 1978. A boundary integral method applied to plate of arbitrary plane form. *Computer and Structures* 9, 283–305.
- Beskos, D.E., 1991. *Boundary Element Analysis of Plate and Shells*. Springer-Verlag, Berlin.
- Bezin, G., 1991. A boundary integral equation method for plate flexure with conditions inside the domain. *Int. J. Numer. Methods. Engng* 17, 1647–1657.
- Du, Q.H., Lu, X.L., 1986. Some further works for the Kirchhoff plate bending problems by highly conforming boundary element method. In: Tanaka, M., Brebbia, C.A. (Eds.), *Boundary Elements VIII*. Springer Verlag, Berlin, pp. 475–485.
- Durbin, F., 1974. Numerical inversion of Laplace transforms: an efficient improvement to Dubner and Abate's method. *Comput. J* 17 (4), 371–376.
- Fedelinski, P., Aliabadi, M.H., Rooke, D.P., 1995. A single-region time domain BEM for dynamic crack problems. *International Journal of Solids and Structures* 32, 3555–3571.
- Hadamard, J., 1923. *Lectures on Cauchy's Problem in Linear Partial Differential Equations*. Yale University Press, New Haven.
- Isida, M. (1977). Interaction of arbitrary array of cracks in wide plates under classical bending, G.C., Sih (Ed.), *Plates and Shells with Cracks*, pp. 1–42.
- Jaswon, M.A., Maiti, M., 1968. An integral equation formulation of plate bending problems. *J. Engng. Math* 2, 83–93.
- Maiti, M., Chakrabarty, S.K., 1974. Integral equation solutions for simply supported polygonal plates. *Int. J. Engng. Sci* 12, 793–806.
- Sih, G.C. and Chen, E.P. (1977). Dynamic analysis of cracked plates in bending and extension, G.C., Sih (Ed.), *Plates and Shells with Cracks*, pp. 231–271.
- Stern, M., 1981. A general boundary integral formulation for the numerical solution of plate bending problems. *J. Solids Struct* 15, 769–782.
- Tottenham, H., 1979. The boundary element method for plates and shells. In: Banerjee, P.K., Butterfield, R. (Eds.), *Development in Boundary Element Methods-I*. Applied Science Publications, London.
- Vander Weeën, F., 1982. Application of the boundary integral equation method to Reissner's plate model. *Int. J. Numer. Methods Engng* 18, 1–10.
- Wen, P.H., 1996. *Dynamic Fracture Mechanics: Displacement Discontinuity Method*. Computational Mechanics Publications, Southampton UK and Boston USA.
- Wen, P.H., Aliabadi, M.H., Rooke, D.P., 1996a. The influence of elastic waves on dynamic stress intensity factors (two-dimensional problems). *Arch. Appl. Mech* 66, 326–355.
- Wen, P.H., Aliabadi, M.H., Rooke, D.P., 1996b. The influence of elastic waves on dynamic stress intensity factors (three-dimensional problems). *Arch. Appl. Mech* 66, 385–394.